The largest stress variations were related to the effects of temperature and particularly to direct exposure to the sun. As the sun passed over the bridge, the exposed surface of the south and then the north tie girder absorbed substantial heat. The maximum measured temperature was 144°F and occurred on the top flange of the south tie girder on July 16, 1979, when the ambient temperature was 90°F. Surfaces not exposed to the sun were always close to the ambient temperature. Temperature differentials of 50°F between the top and bottom flange plates and 20°F between the outside and inside web plates were measured in both tie girders.

The strain measurements indicated that the state of stress in the tie girders in the vicinity of the arch ribs is very complex. Maximum daily stress ranges in the longitudinal direction of the tie girders were about 10 ksi on the hot days. Where local bending occurred in the web plates, the maximum daily stress ranges were about 20 ksi.

Strain readings on two days of similar temperature conditions were compared in an effort to estimate the underlying stress variation due to light and heavy traffic. These days were Sunday, July 15, and Tuesday, July 17. Gages on section NB and strain gage NF1 were selected for the comparison. Readings were compared between 2:00 and 6:00 p.m. Most of the differences in stress are less than 1 ksi at section NB. Stress values obtained from gage NF1 show a change of 2 ksi in the web of the tie girder perpendicular to the arch rib. Therefore, the underlying stress variation due to traffic is believed to be about 1-2 ksi.

Because the density of the traffic may vary even during peak periods, it is thought that the underlying stress variation due to traffic should be considered to occur, at most, 50 times a day. This variation combines with the stress ranges associated with the passage of heavy vehicles.

CONCLUSIONS

Field testing indicated that stress ranges in the tie girders under traffic were generally less than 2 ksi and only infrequently 3 ksi. The number of cycles varied with the location, but it did not exceed the ADTT. However, the temperature of plates exposed to the sun may be as much as 50°F higher than the temperature of plates in the shade, which is always close to the ambient temperature. The nominal stress may change by about 10 ksi as a result of daily thermal effects. Where local bending was present, the daily stress range was about 20 ksi.

ACKNOWLEDGMENT

The field test discussed in this paper was part of a larger study conducted under the overview of a technical committee that included chairman Walter J. Hart and John C. Jenkins of OSHD and Carl Hartbower, Herbert A. Schell, and Frank Sears of the Federal Highway Administration.

Wiss, Janney, Elstner and Associates, Inc. (WJE), was assisted in the study by the following consultants and subcontractors: John W. Fisher of Lehigh University; Ammann and Whitney; Materials Research Laboratory, Inc.; and Testing Engineers, Inc. Other members of the WJE project staff included Boris Bresler, Robert Iding, and Daryl W. Boggs.

REFERENCES

1. J.M. Hanson, M.J. Koob, and B. Bresler. Post-Construction Evaluation Study, Fremont Bridge (Willamette River), I-405-Bridge 2529. Oregon State Highway Division, Salem, Dec. 30, 1981, 181 pp.
2. A. Hedefine and L.G. Silano. Design of the Fremont Bridge. ASCE National Structural Engineering Meeting, Portland, OR, Preprint 1210, April 1970.

Publication of this paper sponsored by Committee on Dynamics and Field Testing of Bridges.

Seismic Design of Curved Box Girders

C.P. HEINS AND I.C. LIN

The seismic response of single and continuous curved steel composite box girder bridges has been predicted by an equivalent structure load method. This method has been developed by computing equivalent structural stiffnesses of the entire bridge for the three displacement directions (x, y, z) and rotation. These stiffnesses are then used to evaluate corresponding natural frequencies (ω_x, ω_y, ω_z, and ω_t) by using a single degree of freedom system. The induced accelerations are then determined from the response spectrum curves. The results of these analyses are then used to develop a series of empirical equations for direct design.

As a result of the 1964 Alaskan earthquake, the 1971 San Fernando earthquake, and, more recently, the 1978 Santa Barbara earthquake (1), bridge structures in the United States have undergone considerable destructive forces. These earthquakes caused bridge professionals to reassess the design techniques that had been applied until that time for seismic design.

A prime force in such modifications has been the California Department of Transportation (Caltrans) and the California-based professional organization, Applied Technology Council (ATC). The present 1977 American Association of State Highway and Transportation Officials (AASHTO) bridge code (2), as related to seismic design, was greatly influenced by the work developed by Caltrans. This code suggests an equivalent static force method for simple structures and, when the structure is complex--as in curved bridges, for example--a computer-based response spectrum or dynamic analysis should be considered.

In the present 1977 AASHTO code, most engineers would use the seismic coefficient method (SCM) because computer-oriented dynamic programs may not be available or are not amenable for direct design. However, the SCM may give erroneous results when used for design under seismic conditions (3), as experienced by Caltrans. Caltrans in fact has used

the response spectrum technique for the design of many structures.

Because of these conditions and experience gained from recent earthquakes, the Federal Highway Administration (FHWA) decided to reassess the 1975 AASHTO code and in 1977 sponsored a research program directed by ATC (4). Part of the work of this council is to prepare a new specification (5). Although this code will be an improvement over past criteria, major areas of research still require investigation. These areas, as suggested recently by delegates attending a workshop conducted by ATC (6), include the following:

1. Conduct of parametric studies for the seismic response of common types of bridges to determine the effects of geometry and constraint on overall seismic response (parameters should include span length, curvature, column height and stiffness, material, etc.),
2. Performance of appropriate dynamic analysis on curved bridges (7,8) and development of a simple procedure for the design of curved bridges,
3. Development of a practical and accurate method to estimate the fundamental period of bridges,
4. Correlation of vibrational characteristics of existing bridges with theory, and
5. Preparation of a summary of dynamic behavior and characteristics.

These areas of research are currently being studied and will encompass curved steel and concrete box girder bridges.

Three techniques can be used in the dynamic analysis of such structures: (a) the response spectrum technique, (b) multimodal method-response spectrum, and (c) multimodal time history analysis. These methods are now being used in this research. The method that was used in the work described in this paper involves a space frame analysis of the general structure, computation of the equivalent natural frequency, and then determination of the equivalent dynamic forces for curved steel composite box girder bridges.

As this paper demonstrates, a comprehensive study of the influence of the various parameters has resulted in a proposed equivalent static load analysis technique. It should be noted that a more comprehensive study is being done that includes time history response and multimodal analysis. These results will then be compared with the results obtained by using the single degree of freedom (SDOF) system and the response spectrum data given here.

THEORY

Computer Model

The general static response of curved bridge structures requires incorporation of the interaction between the bending and torsional forces (7-12). Such interaction can be considered by solving Vlasov equations (12) or by development of the stiffness matrix (13) and appropriate restraint conditions.

The matrix-oriented technique, however, is more versatile in that a three-dimensional model (space frame) can be considered. This then permits modeling of the structure so that the support conditions can represent the physical restraints. In addition, the induced actions can be applied in three directions and thus simulate the various earthquake-induced actions.

Therefore, the study of the induced actions on a structure subjected to earthquakes was confined to the use of a space frame matrix simulation. The basic modeling consists of a series of typical elements attached rigidly together to form a continuous curved box girder bridge.

The basic properties of each beam element consist of I_z, I_y, and K_T. Although warping and distortional properties (I_w, W_n, and W_a) can be computed, they were not considered in this study because it has been shown that, with proper bracing of the box girder, warping and distortional effects are negligible (10).

Therefore, by properly evaluating the stiffness of each beam element and identifying each joint load, the static response of the continuous curved girder can be determined. The static response can then be used to determine the effective earthquake effects by using the response spectrum curves. The general procedure in which this method is used can now be described.

The support restraints to be imposed on the bridge model can be identified as releases in the computer model. Because a space frame model is being used, six releases or restraints must be identified. For the bridge under study, the following was assumed.

Equivalent Dynamic Analysis

The natural frequency response (ω) of an SDOF system can be predicted by the following (14-17):

$$\omega = \sqrt{k/m} \tag{1}$$

where k is the spring constant and m is mass [w/g (total weight of structure/gravity)] or mass moment of inertia.

If the frequency ω of the system, as computed from Equation 1 or some other technique, is reliable, then the corresponding induced vertical acceleration of the mass m created by an earthquake can be predicted by using the response spectrum curves given in Figures 1-3. The accelerations obtained are then used to determine the induced dynamic force:

$$F = m \cdot a_{RS} \tag{2a}$$

where $a_{RS} = \ddot{y}$ = linear acceleration obtained from response spectrum curves (18).

If the system is subjected to angular accelerations $\ddot{\theta}$, then the induced dynamic torque (M) is

$$M = \bar{I}\ddot{\theta}_{RS} \tag{2b}$$

where

$\bar{I}$ = mass moment of inertia = $\int pr^2 dA = \rho_{steel} \int (x^2 + y^2)dA + \rho_{concrete} \int (x^2 + y^2)dA$,
$\ddot{\theta}_{RS}$ = rotational acceleration obtained from the response curve (19), and
ρ = mass per unit area.

This type of procedure has been proposed elsewhere (3-7,18,20-25) and requires a methodology that can accurately determine the natural frequency (ω) of the structure.

Natural Frequency

As indicated by Equation 1, the natural frequency of an SDOF system is given as a function of the spring stiffnesses (k) and the spring mass (m). If the system is a bridge structure, the spring constant can be represented by

$$k = (1/\Delta) \tag{3}$$

where Δ is the induced maximum displacement caused

by a unit load. Therefore, by determining the response of a given box girder bridge when subjected to a unit load, an equivalent spring constant can be obtained. This constant (k) and the total mass of the bridge will then permit evaluation of the natural frequency as given by Equation 1.

In the instance of curved structures, the dynamic action can occur in three principal directions and one primary rotation. The resulting maximum displacement induced by these unit loads will then give the corresponding equivalent stiffnesses (k_x, k_y, k_z, and k_T) as shown in Figure 4. The corresponding natural frequencies can then be determined by applying Equation 1.

Computer Program

A general computer program has been developed (26) that will automatically determine the equivalent spring constant for the three translation directions (k_x, k_y, and k_z) and the one rotation (k_T) of a continuous, constant-radius bridge. Section properties are automatically computed and are used for determination of the stiffness matrix. Dead

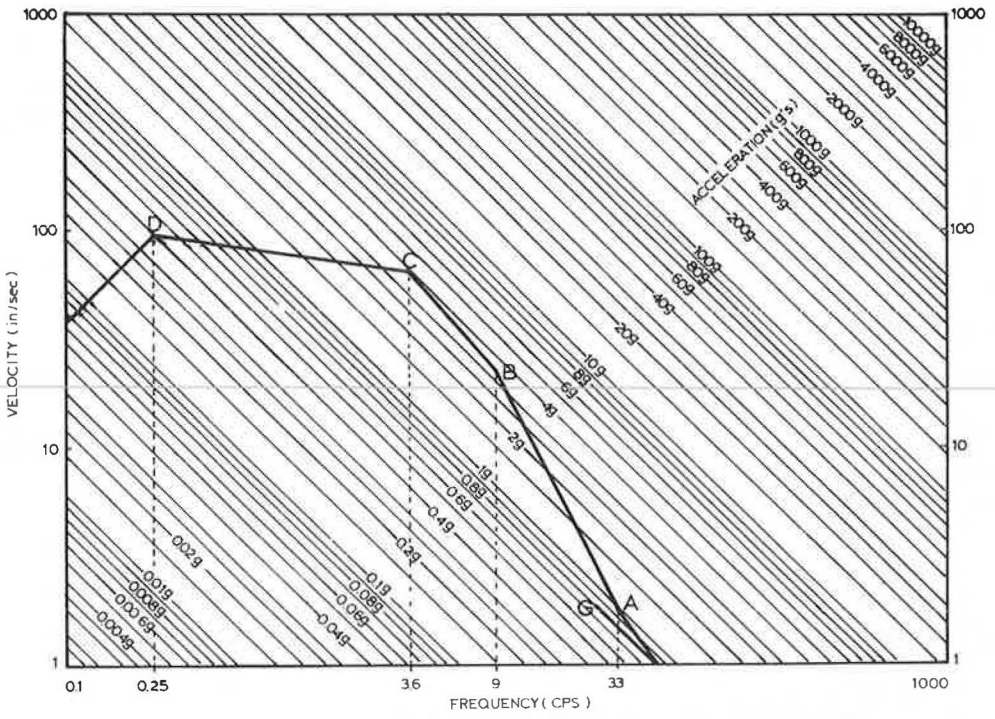

Figure 1. Vertical response spectrum for 1.0-*g* maximum ground acceleration.

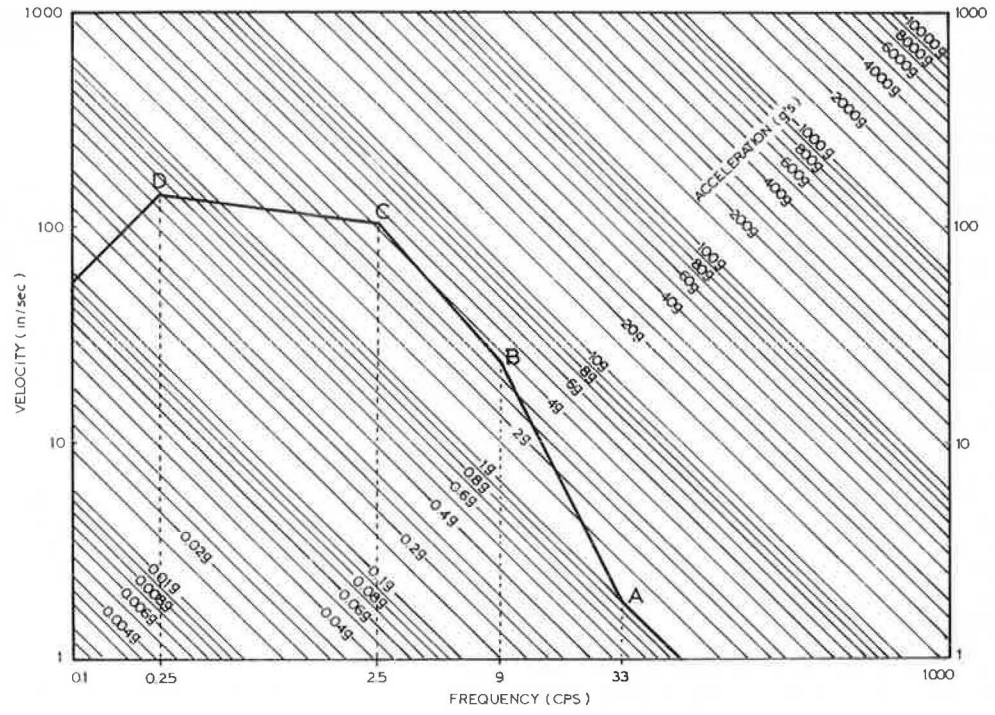

Figure 2. Horizontal response spectrum for 1.0-*g* maximum ground acceleration.

loads and masses are also computed and are used to determine the equivalent dynamic force, as given by Equation 2. This dynamic force is then applied uniformly to the structure, and the resulting deformations and actions are determined.

The response spectra (Figures 1-3) have also been incorporated into the program for direct use. Based on a constant 2 percent damping value for these types of bridges (18,22), the general curves have been written in algebraic form (26).

Figure 3. Torsional response spectrum.

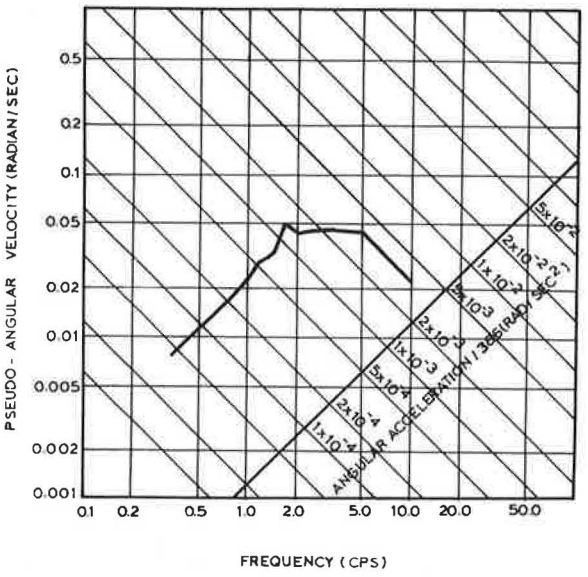

The program will automatically select 11 nodes for each span with 10 members/span between the supports. The proper member properties corresponding to the basic input section lengths are automatically determined. The interior support restraints are assumed to be flexible due to the insertion of springs in the three displacement directions.

BRIDGE STUDIES

Typical Sections

In order to develop a simplified design technique, the response of various curved box girder bridges must be examined. Such box girders, which have been used in previous studies (7), were used in this parametric study. Only the three-lane, three-girder system was considered in this study because this is most typical of curved box girder structures (10).

The basic span length configurations examined are shown in Figure 5, where length (L) = 50-150 ft and N (ratio of span length) = 1.2. The radius used for these various structures varied from 200 ft to infinity.

Column Details

In order to include the influence of the flexibility of the piers, a survey was conducted to determine typical pier configurations and sizes. Such a survey has indicated that for a roadway of 44 ft, with three boxes, a three-column bent is generally used. Such column bents generally have the following details:

Column		Steel Bars	
Type	Size (ft)	Type	No.
Round	$2.5 \leq d \leq 3.0$ (diameter)	#11	12-20
Rectangular	4x12	#8 or #9	30-40

Figure 4. Equivalent structural stiffness.

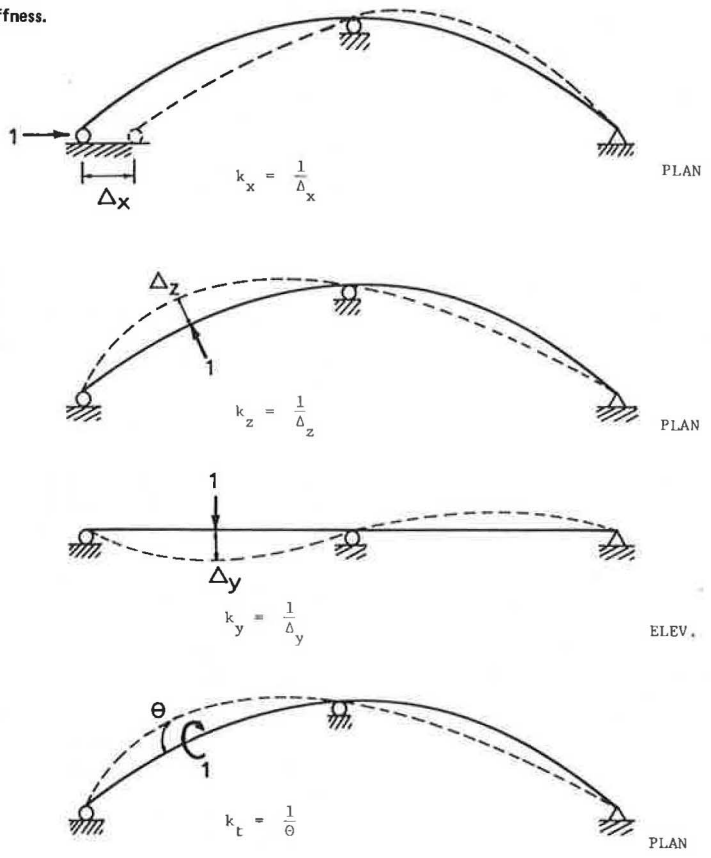

Figure 5. Modeled bridge details.

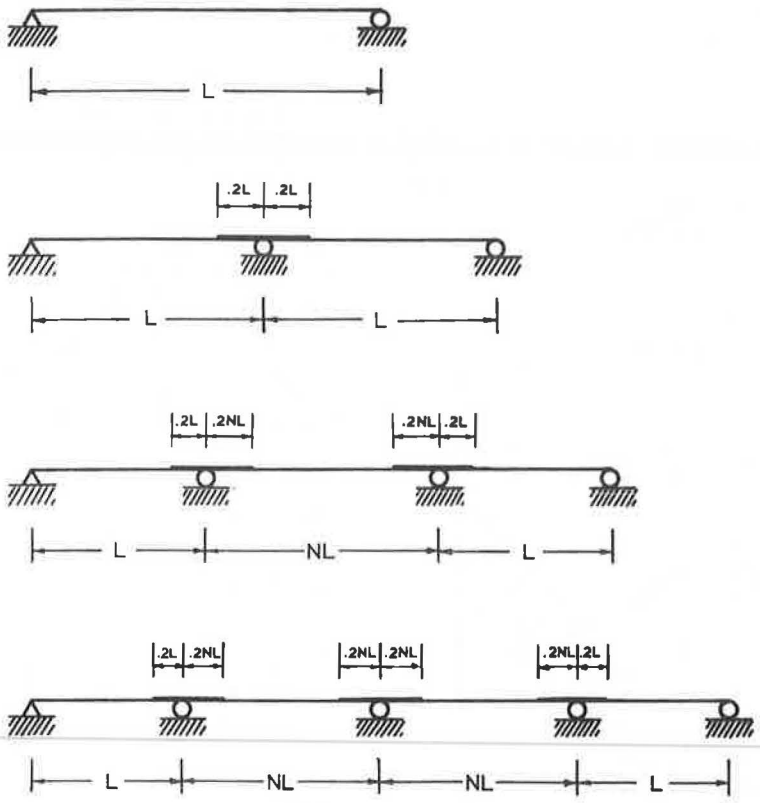

The height of the bents is 10-15 ft, and the spacing between columns is 15-18 ft.

By using this basic information, the section properties (I_x and I_z) of the round and the rectangular column have been computed (26).

These column stiffnesses were used and a three-column bent type was assumed in determining the deformation of the bent caused by a unit load in the transverse and longitudinal directions (with rigid pier caps). The equivalent spring constant was then determined from

$$k_z = (1/\Delta) = [L^3/3E(3I_x)] \quad (4)$$

$$k_x - (1/\Delta) = [L^3/3E(3I_z)] \quad (5)$$

The resulting k_z and k_x values for the column heights of 10 and 15 ft were then determined (26).

With these equivalent pier stiffnesses, the internal piers can then be modeled by using equivalent springs.

General

By using the basic box geometry and the support spring constants of $k_x = 0\text{-}2\text{x}10^3$ kip/in, $k_y = \infty$, and $k_z = 0.5\text{x}10^3$ kip/in to ∞, the equivalent seismic responses of the single-, two-, three-, and four-span structures were examined. The resulting natural frequencies (ω_x, ω_y, ω_z, and ω_t) for all bridge spans and their corresponding induced accelerations were then obtained (26). For the continuous spans, the pier flexibilities, as given by k_x and k_z, were also included as a variable. Three basic variations have been assumed:

1. $k_x = 0$, k_z = rigid;
2. $k_x = 0.66 \times 10^3$ kip/in, $k_z = 0.5 \times 10^3$ kip/in; and
3. $k_x = 2 \times 10^3$ kip/in, $k_z = 0.66 \times 10^3$ kip/in.

The analyses of the various bridges have been performed and have resulted in typical response curves for ω_x, ω_y, ω_z, and ω_t as a function of radius (R) and L. An example of such a response (ω_x) for a two-span structure is shown in Figure 6.

The induced accelerations, as determined from the response spectra, have also been plotted as a function of L/R and L for the single span (26).

However, the corresponding accelerations for the continuous spans and the single span have been plotted in Figure 7 as a function F versus the number of spans, radius, stiffnesses (k_x and k_z), and span lengths, where

$$F_x = A_x \text{ (continuous-span value)}/A_x \text{ (single-span value)} \quad (6)$$

For all span lengths of 50, 100, and 150 ft, similar relations between F_y, F_z, and F_t have been plotted (26). These data were then used to develop appropriate design criteria.

MULTIMODAL SOLUTIONS

To demonstrate the reliability of this simulated dynamic solution, the response of single-span and multispan bridges with rigid and flexible column bents has been examined by using the SAP IV computer program (13). This program idealizes the bridge as a three-dimensional unit and examines dynamic response by using dynamic mass matrix techniques.

Examination of the dynamic response of a three- and four-span continuous curved structure on flexible bents has resulted in the data (ω_x, ω_y, ω_z, and ω_t) given in Table 1. Examination of these data indicates that the comparisons between the resulting frequencies obtained from the space frame structure and SAP IV are reasonable but that only the ω_x and ω_y values are in agreement. It should be noted, however, that the SAP IV solu-

Figure 6. Natural frequency (ω_x) versus radius for two-span bridges.

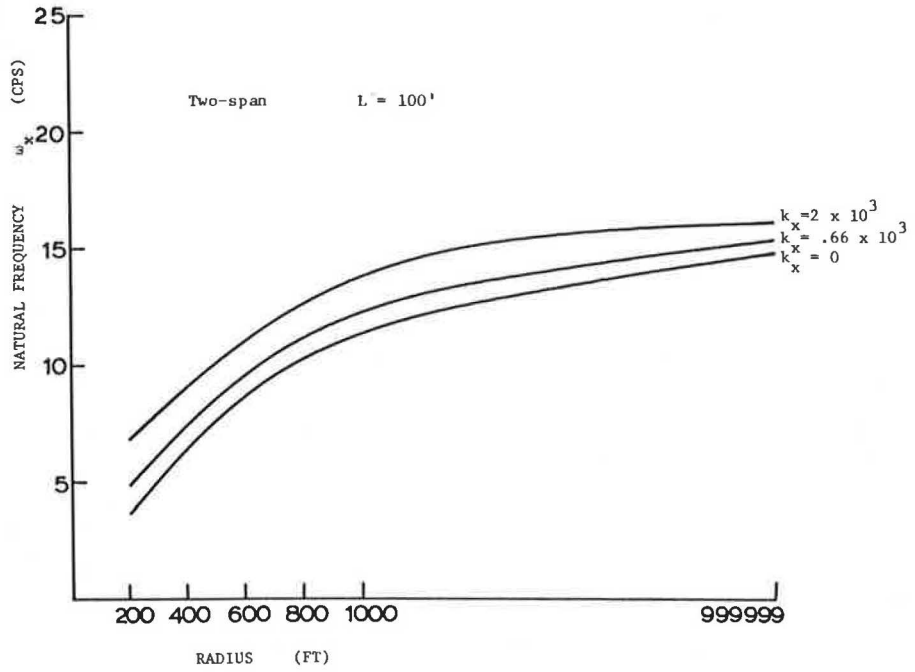

Figure 7. Continuity factor F_x versus number of spans (L = 50 ft).

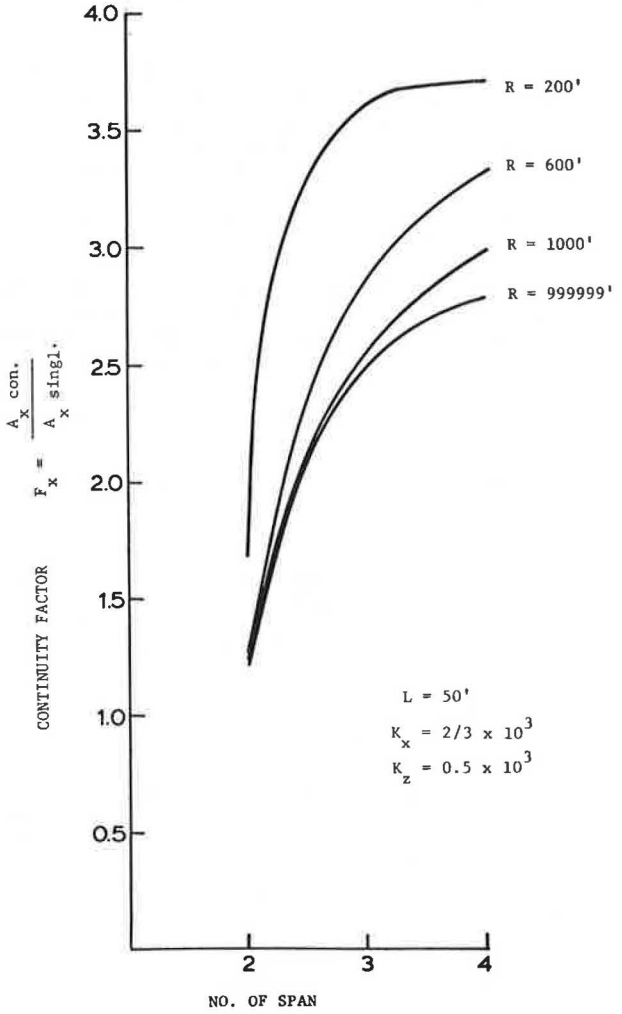

tion does not provide for the angular frequency (ω_t) and, if one compares the ω_t obtained from the space frame structure with ω_z, there is excellent agreement. Therefore, it is reasonable to assume that the space frame structure that gives ω_z and ω_t is a combination of the data given by ω_z obtained from SAP IV.

DESIGN CRITERIA

Trends

The seismic design of continuous curved box girders will be related to the response of single-span curved girders. Therefore, the single-span accelerations (A_x, A_y, A_z, and A_t) were determined with respect to the basic bridge geometry, which yielded the following:

A_x for 100 ft < L ≤ 150 ft = 2.2 $(L/R)^2$ + 0.011L + 0.45 (7)

A_y for L ≥ 100 ft = - 0.016(L) + 4.7 (8)

A_z for L ≥ 100 ft = 3.8 (9)

A_t for L ≥ 100 ft = 1.5 (10)

The continuity factors F have similarly been determined in analytic form. This results in the following four continuity factors:

F_x (longitudinal) = - 0.02(L) + 3.75 + K (11)

where K = 0.00125R for R ≤ 600 ft and K = 1.0 for R > 600 ft.

F_y (vertical) = -0.125(NS) - 0.002L + 1.35 (12)

where NS is the number of spans (2, 3, or 4).

F_z (transverse) = -0.005L + 1.5 (13)

F_t(torsion) = -0.075(NS) + 1.15 (14)

Table 1. SDOF solution (space frame) versus SAP IV.

Type of Structure	ω_x (cycles/s)		ω_y (cycles/s)		ω_z (cycles/s)		Space Frame ω_t (cycles/s)
	Space Frame	SAP IV	Space Frame	SAP IV	Space Frame	SAP IV	
Three span where L = 150, 180, and 150 ft and R = 100 ft	3.682	4.282	1.129	1.823	1.189	4.715	4.506
Four-span where L = 150, 180, 180, and 150 ft and R = 1000 ft	3.5232	3.444	0.966	1.639	1.016	3.950	3.855

Design Approach

The equivalent seismic design of curved box girder bridges will incorporate the primarily developed equations and the effective peak acceleration map (K_p) given by AASHTO (2). The general design equations for translation and rotation, respectively, are of the following form

$$EQ_n = F_n \cdot A_n \cdot m \cdot K_p \quad (15)$$

$$EQ_n = F_n \cdot A_n \cdot \bar{I} \cdot K_p \quad (16)$$

where

EQ_n = total applied seismic force in x, y, z, or t directions;
F_n = continuity factor in x, y, z, or t directions;
A_n = single-span acceleration;
K_p = effective peak acceleration modifying factor (2); and
$\bar{I}$ = rotational mass moment of section = $\rho\int(x^2 + y^2)dA$.

For the specific direction n, the continuity factor F and single-span acceleration A_n are given by Equations 7-14.

SUMMARY AND CONCLUSIONS

The seismic response of single and continuous curved steel composite box girder bridges has been predicted by an equivalent structure load method. This method has been developed by computing equivalent structural stiffnesses of the entire bridge for the three displacement directions (x, y, and z) and rotation. These stiffnesses are then used to evaluate corresponding natural frequencies (ω_x, ω_y, ω_z, and ω_t) by using an SDOF system. The induced accelerations are then determined from the response spectrum curves. The results of these analyses are then used to develop a series of empirical equations for direct design.

ACKNOWLEDGMENT

The work covered in this paper has been supported by a grant from the National Science Foundation. The support, encouragement, and guidance of the National Science Foundation are gratefully acknowledged.

REFERENCES

1. R.K. Miller and S.F. Felszeghy. Engineering Features of the Santa Barbara Earthquake of August 1978. Earthquake Engineering Research Institute, Berkeley, CA, 1978.
2. Standard Specifications for Highway Bridges, 11th ed. AASHTO, Washington, DC, 1973.
3. R.A. Imbsen, R.V. Nutt, and J. Penzien. Evaluation of Analytical Procedures Used in Bridge Seismic Design Practice. Proc., Workshop on Earthquake Resistance of Highway Bridges, Palo Alto, CA, Jan. 29-31, 1979.
4. R.L. Sharpe and R.L. Mayes. Development of the Highway Bridge Seismic Design Criteria for the United States. Proc., Workshop on Earthquake Resistance of Highway Bridges, Palo Alto, CA, Jan. 29-31, 1979.
5. Seismic Design Guidelines for Highway Bridges. Applied Technology Council, Berkeley, CA, ATC-6, Oct. 1981.
6. R.L. Sharpe and R.L. Mayes, eds. Proceedings of Workshop on Earthquake Resistance of Highway Bridges, Palo Alto, California, Jan. 29-31, 1979. Applied Technology Council, Berkeley, CA, 1981.
7. C.P. Heins and M.A. Sahin. Natural Frequency of Curved Box Girder Bridges. Journal of Structural Division, ASCE, Vol. 105, No. ST12, Dec. 1979.
8. C.P. Heins and R.S. Humphreys. Bending and Torsion Interaction of Box Girders. Journal of Structural Division, ASCE, Vol. 105, No. ST5, May 1979.
9. C.H. Yoo and C.P. Heins. Plastic Collapse of Horizontally Curved Bridge Girders. Journal of Structural Division, ASCE, Vol. 98, No. ST4, April 1972.
10. C.P. Heins. Box Girder Design: State of the Art. Engineering Journal, American Institute of Steel Construction, Vol. 15, No. 4, 1978.
11. C.P. Heins and D.A. Firmage. Design of Modern Steel Highway Bridges. Wiley-Interscience, New York, 1979.
12. C.P. Heins. Bending and Torsional Design in Structural Members. Lexington Books, Heath, Lexington, MA, 1975.
13. K. Bathe, E. Wilson, and F. Peterson. SAP IV: A Structural Analysis Program for Static and Dynamic Response of Linear Systems. Department of Civil Engineering, Univ. of California, Berkeley, June 1973.
14. N.M. Newmark and E. Rosenblueth. Fundamentals of Earthquake Engineering. Prentice-Hall, Englewood Cliffs, NJ, 1971.
15. D.J. Dowrick. Earthquake Resistant Design. Wiley, New York, 1977.
16. R.W. Clough and J. Penzien. Dynamics of Structures. McGraw-Hill, New York, 1975.
17. R.L. Wiegel. Earthquake Engineering. Prentice-Hall, Englewood Cliffs, NJ, 1970.
18. R.R. Robinson and others. Structural Analysis and Retrofitting of Existing Highway Bridges Subjected to Strong Motion Seismic Loading. FHWA, May 1975.
19. W.K. Tso and T.-I. Hsu. Torsional Spectrum for Earthquake Motions. Earthquake Engineering and Structural Dynamics, Vol. 6, Oct. 1977.
20. D. Williams and W. Godden. Effectiveness of Existing Bridge Design Methodology in Resisting Earthquakes: Phase IV. FHWA, Rept. FHWA-RD-77-91, June 1976.
21. H.E. Chapman. An Overview of the State of Practice in Earthquake Resistant Design of Bridges in New Zealand. Proc., Workshop on Earthquake Resistance of Highway Bridges, Palo Alto, CA, Jan. 29-31, 1979.
22. R.R. Robinson, A. Longinow, and K.H. Chu.

Seismic Retrofit Measures for Highway Bridges. FHWA, Rept. FHWA-TS-216, Vol. 1, April 1979.
23. T. Iwasaki. Earthquake Resistant Design of Bridges in Japan. Ministry of Construction, Tokyo, Vol. 29, May 1973.
24. M. Ohashi, E. Kuribayashi, T. Iwasaki, and K. Kawashima. An Overview of the State of Practices in Earthquake Resistant Design of Highway Bridges in Japan. Presented at Workshop on Research Needs of Seismic Problems Related to Bridges, San Diego, CA, Jan. 1979.
25. N. Yamadera and Y. Oyema. Special Considerations and Requirements for Seismic Design of Bridges in Japan. Metropolitan Expressway Public Corp., Tokyo, n.d.
26. I.C. Lin. Equivalent Seismic Design of Curved Box Girder Bridges. Department of Civil Engineering, Univ. of Maryland, College Park, M.S. thesis, April 1981.

Publication of this paper sponosred by Committee on Dynamics and Field Testing of Bridges.

Test to Failure of the Hannacroix Creek Bridge

DAVID B. BEAL

A 52-year-old reinforced concrete T-beam bridge was destructively tested to evaluate the consequences of concrete deterioration on load capacity. Instrumentation included measuring tension and compression rebar strain at midspan, end rotation, and midspan deflection. The single- and double-T test specimens were loaded symmetrically to produce a constant-moment region at midspan. The condition of the bridge was rated 2.5 on a scale from 1 (potentially hazardous) to 7 (new condition). The concrete deck was highly fractured throughout and the cement paste severely deteriorated locally. Efflorescence was common and leakage was evident. Tension rebars exposed by spalled concrete had lost 1-2 percent of their cross-sectional area. It is concluded that the deterioration noted has no significance with respect to the load-carrying capacity of the structure. Based on theoretical arguments, it is concluded that deterioration sufficient for substantial reduction in the capacity of a structure would be manifested in a local collapse and that overall failure of reinforced concrete T-beam bridges need not be a concern.

National bridge inspection standards require that highway bridges be inspected and rated for load-carrying capacity. For steel structures, the guidelines are straightforward and they can be rated without difficulty. Reinforced concrete bridges, by contrast, are not easily rated because the significance of deterioration may be unquantifiable. Because of this difficulty, in 1978 New York State initiated a research program to develop a low-cost field testing method for evaluating structural strength. This effort was abandoned when, at the load levels attainable, it was shown that bridges with sound and deteriorated concrete did not differ in behavior (1).

Because service-load tests could not show differences attributable to deterioration, a test to failure of a heavily deteriorated bridge was planned. It was believed that correlation of the results of such a test with the findings of a thorough pretest inspection and evaluation would give some insight into quantification of the effects of observable deterioration.

TEST STRUCTURE

The test structure is a reinforced concrete T-beam bridge constructed in 1930 that carries NY-32 over the Hannacroix Creek in Albany County. It consists of seven beams 39.5 in long and a 36-ft clear span between faces of the abutments. Nominal cross-section dimensions and reinforcement details for an interior beam are shown in Figure 1. In addition, a nonstructural 4-in concrete wearing surface and a 3-in asphalt wearing surface were removed before testing. The flexural reinforcement consists of eight 1.25-in-square deformed bars that provide a nominal cross-section area of 12.5 in² for a reinforcement percentage of 2.25. Compression reinforcement is negligible. In the center 21 ft, 10 in, shear reinforcement spacing exceeds the limits set by current specifications (2, p. 78).

The expansion end bearings consist of steel plates separated by a layer of graphite grease. This detail makes no provision for end rotation. At the "fixed" ends, 0.75-in-diameter rods are embedded in the abutment and end diaphragm. The beam ends and diaphragm rest directly on the abutment, a detail that restrains translation and rotation.

Bridge condition at the time of testing was poor. The most recent inspection report rates the primary members at 2-3 on a scale from 1 (potentially hazardous) to 7 (new condition). Figure 2 shows a photo montage of the underside of the structure that, except for slight transverse parallax, reliably shows its condition. Spalled concrete areas exposing the tension rebars in the beam stems are evident. The exposed rebars are rusted but do not appear to have suffered more than 1-2 percent loss of cross-sectional area. Although it is not visible in Figure 2, the vertical faces of all beams exhibited extensive cracking, generally paralleling their axes. Efflorescence (the white areas in Figure 2) is common and leakage is evident.

Cores drilled through the deck showed it to be highly fractured throughout and that the cement paste was severely deteriorated locally. The disintegration of the 4-in concrete wearing surface may be linked to its relatively high absorption (3). Failure of the structural deck concrete is judged to have resulted from the freezing of water in pores of the cement paste, aggravated by the presence of chlorides in solution. Deterioration of the T-beam stems has resulted from the same causes, plus corrosion of the steel reinforcement. These mechanisms are facilitated by increased permeability, presumed to be related to absorption. Mean absorption of seven core segments taken from the structural deck was 5.6 percent. This value is greater than about 80 percent of values measured in cores from other New York bridge decks. The upper 1 in of structural deck was disintegrated and came off with the concrete wearing surface. Thus, the structure was tested with a 6-in slab (see Figure 3).

Sonic pulse-velocity measurements through the stems of beams 3, 4, and 6 yielded values of 1700-4400 ft/s. Although precise correlation of concrete